Statistical characteristics of grain boundary ensembles in variously textured copper

O. V. MISHIN*
Materials Research Department, Risø National Laboratory, DK-4000 Roskilde Denmark
E-mail: oleg.mishin@risoe.dk

Microtextures, misorientation distributions and orientation correlations were investigated in weakly and strongly textured states obtained during recrystallization and grain growth of pure copper. A predominance of $\Sigma 3^n (n \geq 1)$ boundaries was found in the condition with weak texture, while mainly low-angle and $\Sigma 3$ boundaries were observed in the strongly textured state. The influence of texture on the microstructure and misorientation distribution is discussed. The misorientation distribution of nearest neighbours in face centred cubic materials prone to annealing twinning is influenced by the "matrix–twin" orientation correlation. Such a correlation is prominent in copper with a weak texture. The influence of this orientation correlation is significantly reduced in the presence of a strong texture. In strongly textured copper, $\Sigma 3$ boundaries can be divided into two groups: true twin boundaries, i.e. boundaries between a twin and its matrix, and boundaries between a twin and its non-matrix neighbour with an orientation close to the matrix grain. These two groups are characterized by different morphologies of $\Sigma 3$ boundaries and different deviations from the exact twin relationship.

1. Introduction

The misorientation between grains is known to be one of the most important parameters for characterizing grain boundary (GB) geometry. To characterize the grain boundary network in polycrystalline materials, GB misorientation (or character) distributions are widely used. Since misorientations are dependent on grain orientations, it is expected that there might be a relationship between crystallographic texture and grain boundary misorientation distribution. This problem has been exploited in several works, for example [1–4]. Most of these works, however, do not take into account possible orientation correlations between adjacent grains and clustering effects, which may occur in real microstructures.

The grain boundary distributions in annealed face centred cubic (fcc) materials with low and medium values of stacking fault energy are known to be influenced by a strong "matrix–twin" orientation relationship [5]. It has been suggested [6] that the texture has a minor effect on the grain boundary distribution in these materials since similar GB distributions have been revealed in materials with different textures. It is pertinent to mention that strongly textured materials prone to twinning have not been considered there.

In a material with a strong texture, there should be a high fraction of crystallites with similar orientations that form low-angle (near $\Sigma 1$) boundaries. Strongly textured fcc materials have been studied in a number of works [7–10]. In Al–0.3 wt % Mg alloy, a high fraction (55%) of low-angle boundaries has been observed in a strongly textured condition, while states with weaker textures revealed considerably lower fractions of low-angle boundaries [7]. In pure Al, grain growth caused strengthening of the initial texture [8]. The total fraction of low-angle boundaries reached 70%. Correspondingly, the fraction of high-angle boundaries was reduced. A somewhat lower frequency (approximately 37%) of $\Sigma 1$ boundaries was observed in a fibre-textured Al film [9]. Pronounced annealing texture appeared to be a reason for many (approximately 29%) low-angle boundaries in SUPRAL 2004 [10]. All these materials, however, are characterized by relatively high stacking fault energies.

The aim of the present study is to analyse the grain boundary distribution in a material susceptible to annealing twinning with a strong texture developed during recrystallization and grain growth. It is well known that a very strong cube texture in copper and some other fcc materials may be formed using simple thermomechanical treatments. On the other hand, copper is susceptible to annealing twinning and a high frequency of twin boundaries is readily achieved during recrystallization. Recent results [4, 11] provided experimental evidence of the possibility of controlling grain boundary and triple junction distributions by altering the crystallographic texture in pure copper. In this work, the grain boundary ensembles in variously textured copper are presented and discussed in detail. Orientation correlations in this material are investigated here.

* Permanent address: Institute for Metals Superplasticity, Russian Academy of Sciences, Ufa, Russia.

2. Experimental procedure

An ingot of high-purity (99.9995%) copper was used in this experiment. Different thermomechanical treatments were performed to obtain two states with strong and weak textures. The initial ingot was rolled 50% at room temperature and annealed at 773 K for 2 h in a salt bath to provide a weak texture (sample A). A part of this annealed sample was used to generate a strongly textured condition (sample B). Subsequently, it was heavily (95%) rolled and several additional successive annealings at different temperatures (473, 773 and 973 K) were performed to generate a cube texture in the course of recrystallization and to strengthen this texture during grain growth. The rolling plane surface of these samples was polished mechanically and electrochemically, etched in a solution of ammonium peroxidisulfate and studied using both optical and scanning electron microscopy (SEM). The grain size was measured by the linear intercept method, taking into account all crystallites regardless of whether or not they had low-angle or twin misorientations to their neighbours. The mean size of crystallites was about 70 μm in both samples. Local orientations were measured using the electron backscatter diffraction (EBSD) technique in a scanning electron microscope. In sample A, orientations of 304 grains were measured in three different regions (in [11], 164 orientations were analysed in this state). In sample B, 234 orientations were collected in four regions. Misorientations between grains were calculated from these data in terms of axis–angle pairs with minimum equivalent misorientation angles. In all, 708 and 509 misorientations between adjacent grains were considered in samples A and B, respectively. The CSL boundaries were categorized using the Brandon criterion $\Delta\theta_c = 15^\circ\ \Sigma^{-1/2}$ [12]. Macrotextures were studied using a fully automated X-ray goniometer. Sample A revealed a weak, nearly random texture. An extremely strong cube texture and its twin component formed in sample B.

(a)

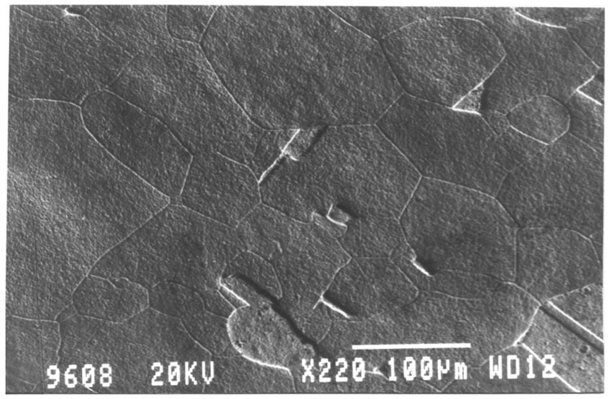

(b)

Figure 1 Microstructures of sample A (a) and sample B (b). Marker is parallel to the rolling direction.

3. Results

Many twins are observed in the microstructure obtained in sample A (Fig. 1a). Straight $\Sigma 3$ boundaries with or without steps are distinguishable in this microstructure. Twins frequently appeared as alternating crystallites with a twin relationship to matrix grains. Orientations of alternating twins were either measured locally in each twin plate or an orientation of a coarser crystallite was ascribed to the extremely fine twin lamellae appearing in the same twin variant within a matrix grain. A fairly uniform distribution of local orientations was obtained in sample A (Fig. 2a).

A strong cube $\{0\,0\,1\}\langle 1\,0\,0\rangle$ texture with a minor twin $\{2\,1\,2\}\langle 1\,2\,2\rangle$ component (Fig. 2b) characterizes sample B. Almost 65% of crystallites had orientations of the cube texture (within 15° from the ideal cube orientation – see Fig. 2c). In this sample, different crystallites contained either few internal twins or did not contain them at all (Fig. 1b). Adjacent cube-oriented grains formed low-angle boundaries; and consequent $\Sigma 1$–$\Sigma 1$–$\Sigma 1$ or $\Sigma 1$–$\Sigma 1$–$\Sigma 1$–$\Sigma 1$ junctions. Within these grains, twins formed straight "matrix–twin" boundaries, with the twin long axis aligned at an angle of approximately 45° to the rolling direction, as observed in the rolling plane (Fig. 1b). When misorientations between adjacent $\{0\,0\,1\}\langle 1\,0\,0\rangle$ grains were sufficiently small, the boundaries between a twin and its non-matrix neighbours belonging to the cube texture (see Fig. 3) also produced the $\Sigma 3$ relationship. Over a relatively long distance, these boundaries revealed some curvature.

While most of $\Sigma 3$ misorientations were close (within 3°) to the ideal 60° $\langle 1\,1\,1\rangle$ twin relationship in sample A, a wide spread of angular deviations, $\Delta\theta$, from the ideal twin relationship was found in sample B. The angular deviations for each $\Sigma 3$ boundary were analysed with regard to its morphology in state B. The deviations for $\Sigma 3$ boundaries normalized with respect to Brandon's maximum angular deviation, $\Delta\theta_c$, for twin boundaries, i.e. 8.66°, are given in Fig. 4 as a function of the GB length. The data presented in Fig. 4 show that there is a significant difference in the deviations from the exact twin relationship for the two groups of $\Sigma 3$ boundaries. Most of the boundaries between twins and their matrix grains were closer to the ideal twin relationship than other $\Sigma 3$ boundaries. The mean $\Delta\theta/\Delta\theta_c$ value was equal to 0.14 and 0.64 for the "matrix–twin" boundaries and boundaries between twins and their cube-oriented neighbours, respectively.

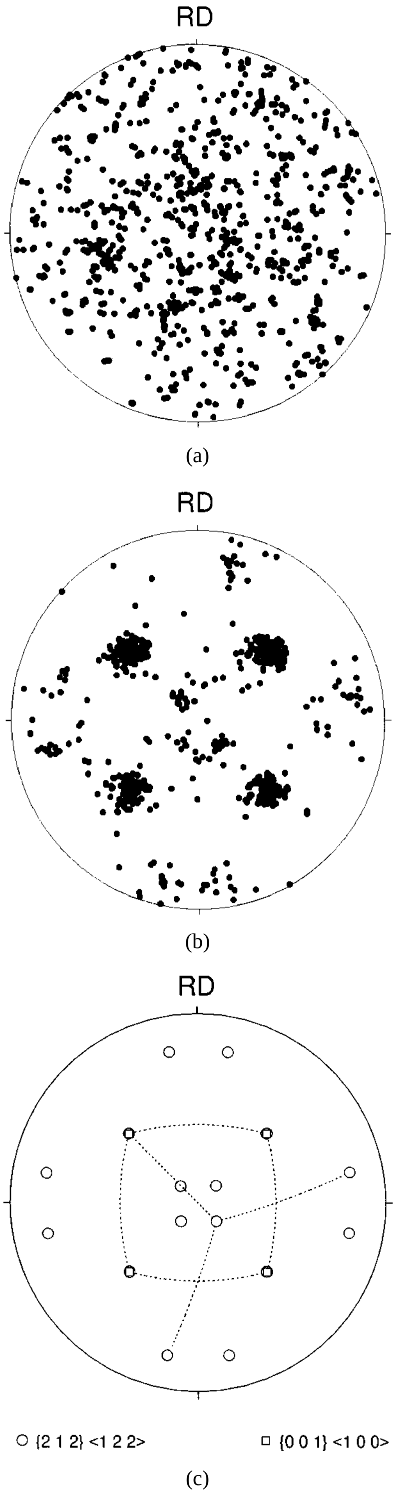

Figure 2 Microtextures of the prepared conditions: (a) sample A; and (b, c) sample B. The ideal positions of the cube $\{0\,0\,1\}\langle 1\,0\,0\rangle$ and $\{2\,1\,2\}\langle 1\,2\,2\rangle$ components are indicated (c).

The distribution of misorientations in two samples is given in terms of distributions by misorientation angles (Fig. 5) and misorientation axes (Fig. 6) within the standard stereographic triangle (SST) divided into the zones according to Mackenzie [13]. A high fraction of misorientations between adjacent grains is concentrated in the vicinity of 60° for sample A (Fig. 5a). Misorientations less than 15° and around 60° are frequent in sample B. In both samples, relatively high fractions of misorientation axes fall into a small zone near the $\langle 1\,1\,1\rangle$ pole of the SST (zone 7 in Fig. 6). The distribution of boundaries by Σ value is shown in Fig. 7. It is seen that the misorientation distribution of the nearest neighbours in variously textured copper are dissimilar primarily in the fractions of Σ1 and Σ3 boundaries. The high frequency of low-angle boundaries distinguished strongly textured condition B from state A with the nearly random texture. In state B, the percentage of low-angle boundaries was nearly an order of magnitude higher compared with condition A. On the other hand, in sample A the total fraction of $\Sigma 3^n (n \geq 1)$ boundaries significantly exceeded the corresponding fraction revealed in the strongly textured sample B.

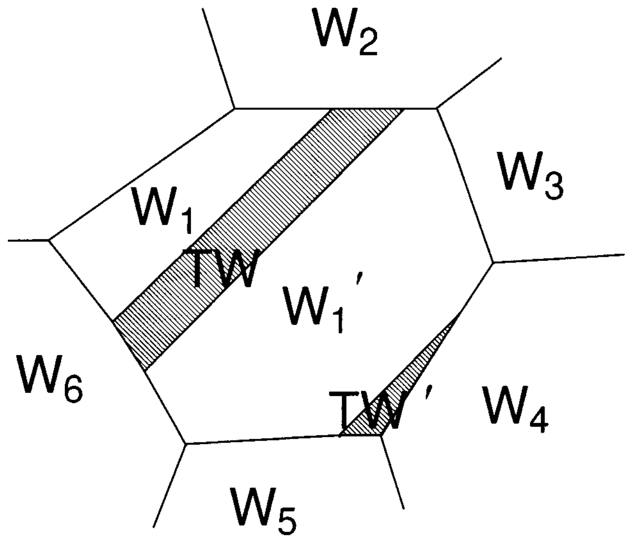

Figure 3 Sketch illustrating possible Σ3 boundaries in strongly textured copper: boundaries W_1–TW, W'_1–TW and W'_1–TW′ are "matrix–twin" (true twin) boundaries; boundaries W_2–TW, W_4–TW′, W_5–TW′ and W_6–TW are "neighbour–twin" boundaries between non-matrix grains and twins. Symbols W and TW denote grains with the cube orientation and its twin component, respectively.

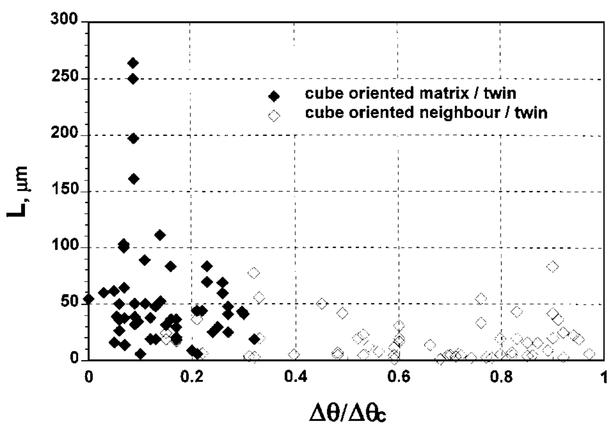

Figure 4 Normalized deviations, $\Delta\theta/\Delta\theta_c$, versus GB lengths, L, for two groups of Σ3 boundaries in strongly textured copper.

To investigate the effect of possible orientation correlations, the distributions of GBs between adjacent grains were compared with those of all mutual misorientations [5, 10, 14]. The mutual misorientations were calculated between all crystallites in each region regardless of whether or not the crystallites were nearest neighbours in the microstructure. Each of N orientations was compared with all other orientations in the inspected region. This gave $N(N-1)/2$ mutual

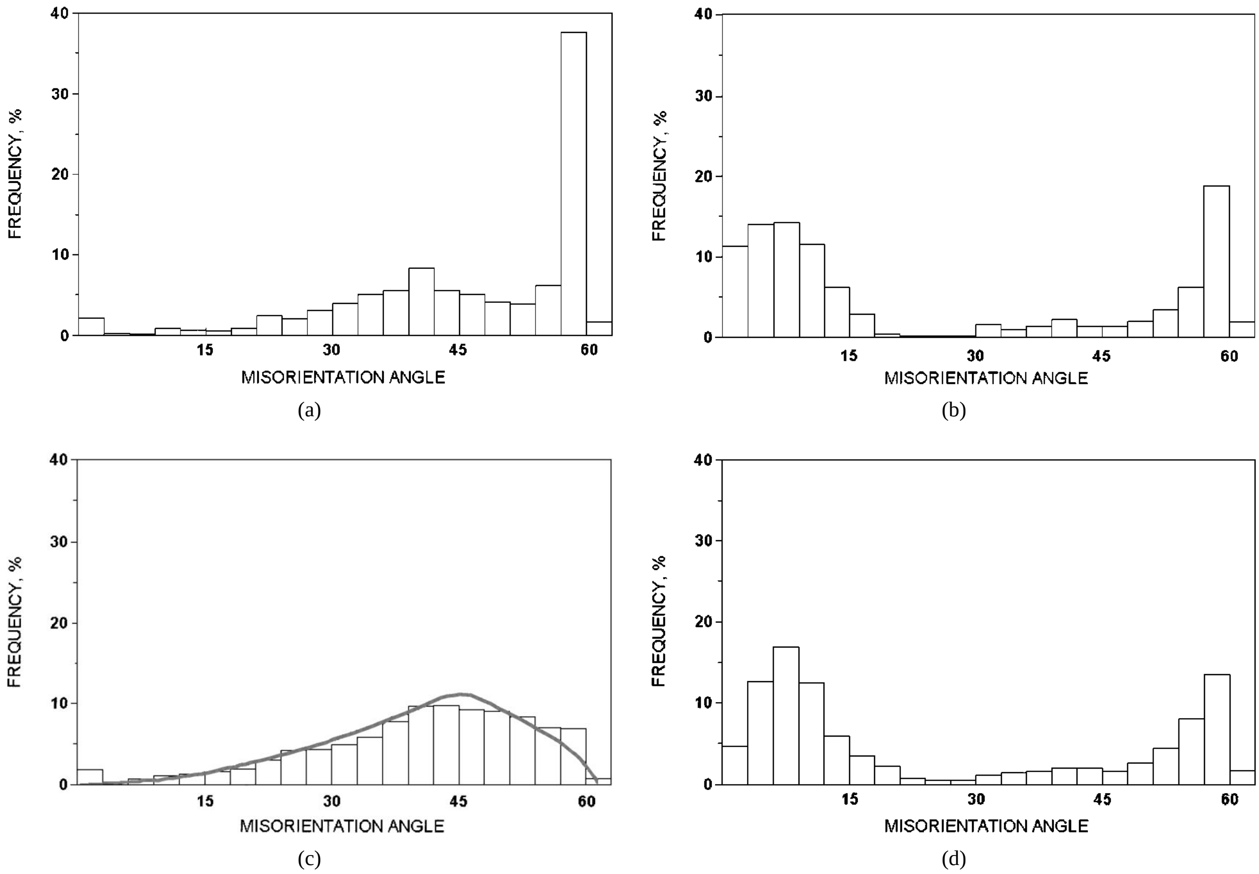

Figure 5 Distributions by the misorientation angles in sample A (a, c) and sample B (b, d); misorientations between nearest neighbours (a, b) and all mutual misorientations (c, d). Solid line (c) corresponds to the misorientation distribution in the random aggregate [15].

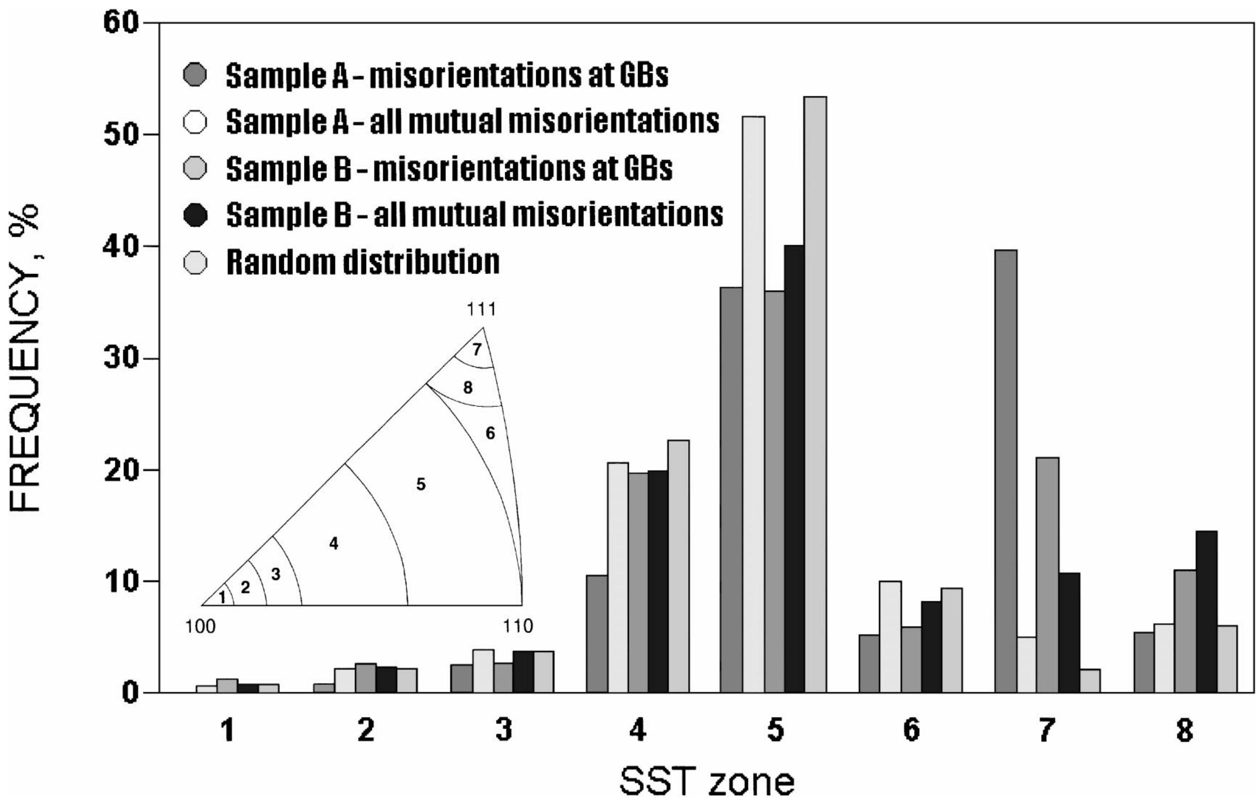

Figure 6 Distribution of misorientation axes within the SST.

misorientations from the data set. The distributions of mutual misorientations were drawn from the cumulative numbers of all mutual misorientations collected from all regions studied in each sample. Figs 5–7 show the differences between the distribution of all mutual misorientations and the misorientation distribution of nearest neighbours in the two states. It is seen that the distribution of all mutual misorientations in

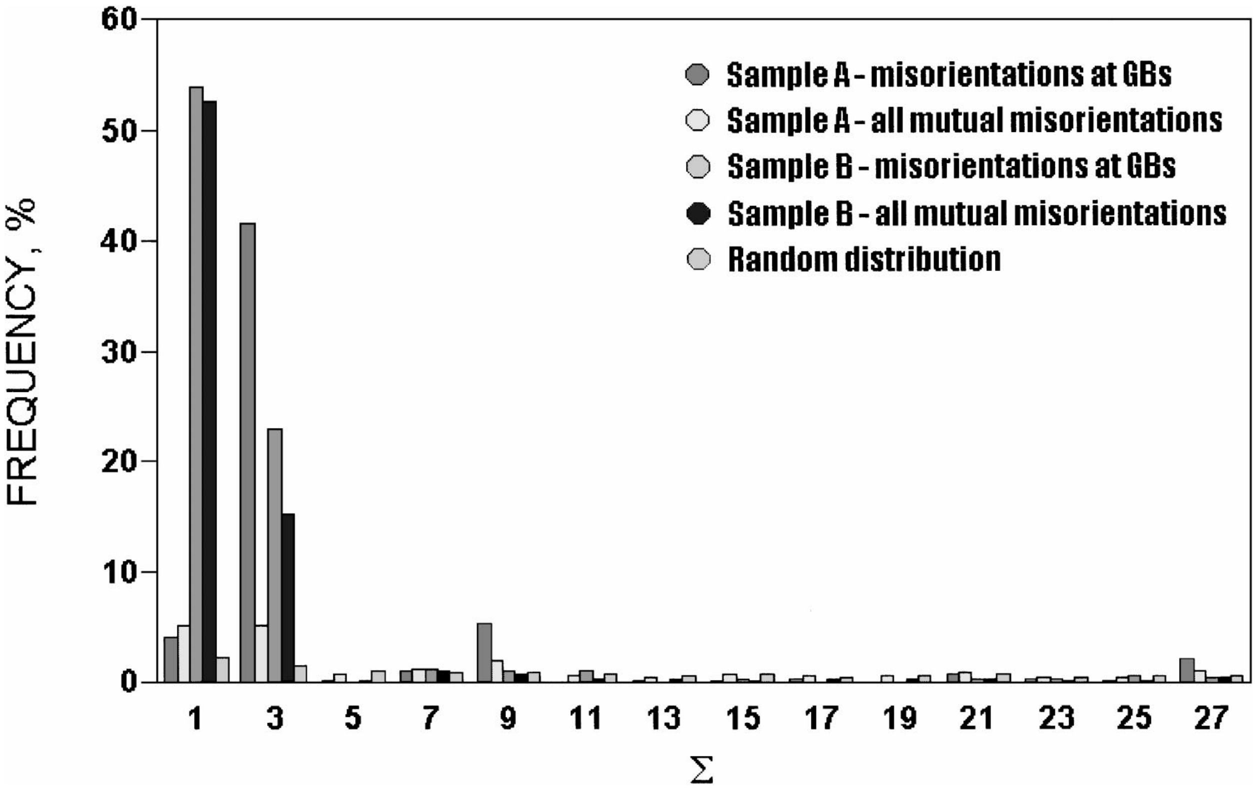

Figure 7 Distribution of grain boundaries by Σ value ($\Sigma \leq 27$).

sample A is similar to the random distribution calculated by Mackenzie [13, 15], while there are no principal differences in the distributions of mutual misorientations and misorientations at GBs in sample B.

4. Discussion

4.1. The influence of texture on GB character distributions

States with similar grain size but significantly different textures revealed quite different distributions of grain boundaries.

In the strongly textured sample B, the total fraction of $\Sigma 3^n$ ($n \geq 1$) boundaries was approximately half that in sample A. Nevertheless, the percentages of Σ3 boundaries were fairly high in both conditions (41.5 and 23% in states A and B, respectively). The predominance of twin boundaries in the misorientation distributions in copper is attributed to the process of annealing twinning. The boundaries of $\Sigma 3^n$ type with $n > 1$ occurred by encounters of twins of different orientations.

The high fraction of low-angle boundaries (54%) in specimen B is obviously connected with the very strong cube texture present in the given condition. A strong cube texture is usually formed in heavily rolled copper during primary recrystallization. Cube-oriented grains have a larger average growth rate during recrystallization [16]. Therefore in the recrystallized state, they are larger than surrounding grains of other orientations, thus producing a pronounced $\{0\,0\,1\}\langle 1\,0\,0\rangle$ texture. Additional annealing leads to the growth of recrystallized $\{0\,0\,1\}\langle 1\,0\,0\rangle$ grains giving rise to their impingement [17]. In such a process grains of similar orientations meet, forming low-angle boundaries. Other grains tend to shrink and disappear, thus resulting in a decrease in the fraction of high-angle boundaries in the misorientation distribution after grain growth [17].

It is noteworthy that in both conditions only boundaries with low Σ values (twin boundaries in sample A or low-angle boundaries in sample B) occurred with higher frequencies after grain growth. Also, increased fractions of CSL boundaries in the presence of strong texture have been reported in Fe–6.5 wt % Si and Ni_3Al [18, 19]. In the present experiment no single high-angle CSL misorientation could be distinguished as occurring more frequently in the strongly textured condition than in sample A. On the contrary, Σ9 and Σ27 boundaries, which could be formed by encounters of twin boundaries, appeared with an increased percentage in weakly textured sample A.

4.2. Orientation correlation effects

The occurrence of low-angle boundaries between nearest neighbours was governed primarily by the volume fractions of closely oriented grains. The fractions of these boundaries between nearest neighbours and of all mutual misorientations were found to be similar in both states (see Fig. 7). However, low-angle boundaries between the nearest neighbours tend to have smaller misorientation angles than those in the distributions of all mutual misorientations in strongly textured copper (Fig. 5b, d).

In the case of weak texture all available orientations appeared in approximately equal proportions and no preferred texture formed. For this reason, crystallites of similar orientations could rarely contact along a common boundary. The distribution of all mutual misorientations in this state is akin to the random Mackenzie distribution [13, 15]. Indeed, in a material with a nearly random distribution of orientations, a misorientation distribution close to the random case could be expected if no orientation correlation between different grains exists, but this has not been observed in materials prone to twinning.

Twin boundaries were reported to appear in high fractions in statically recrystallized stainless steels with different multicomponent textures [6, 20], though their fractions in the distribution of all mutual misorientations were relatively low [5]. Similar results were obtained by Heidelbach *et al.* [21] in annealed copper with multicomponent textures. A great discrepancy in the fraction of $\Sigma3$ boundaries was found by comparison of the GB character distributions calculated between adjacent grains and between randomly selected orientations in annealed nickel with weak textures [22].

Therefore, it is not surprising that the mutual $\Sigma3^n$ misorientations in "textureless" copper were only slightly more frequent than in the random distribution, whereas the frequencies of $\Sigma3$, $\Sigma9$ and $\Sigma27$ boundaries between adjacent grains exceeded greatly the corresponding random fractions. Even in the strongly textured material, where only grains with the cube and its twin components occurred with increased frequencies, $\Sigma3$ boundaries between neighbours appeared more frequently than would be expected excluding any orientation correlation. Also, in sample B, $\Sigma3$ boundaries between neighbours had misorientations closer to the ideal $60^\circ\langle 1\,1\,1\rangle$ twin relationship (compare Fig. 5b with d and the percentage of misorientation axes in the vicinity of the $\langle 1\,1\,1\rangle$ pole of the SST – zone 7, Fig. 6).

The prevalence of twin boundaries between adjacent grains over their frequencies in the distribution of all mutual misorientations is, nevertheless, essentially reduced in the presence of strong texture. The fraction of $\Sigma9$ boundaries in the distribution of neighbours is not much different from that in the distribution of all mutual misorientations. The $\Sigma27$ boundaries constitute low fractions in both these distributions. In sample B, the misorientation distribution of nearest neighbours resembles the distribution of all mutual misorientations. This observation qualitatively agrees with the results of Pan and Adams [9], who compared misorientations across grain boundaries with a computer simulated CSL distribution in a fibre-textured aluminum thin film. Since in a strongly textured material, orientations of available grains occupy a very limited orientation space, there is little opportunity to produce some specific orientation correlations. Strong texture (cube plus twin-to-cube components) in sample B causes the predominance of $\Sigma1$ and $\Sigma3$ boundaries in the misorientation distributions (see Figs 5b, d and 7).

4.3. Characteristics of $\Sigma3$ boundaries in strongly textured copper

In sample A, $\Sigma3$ boundaries are easily recognized by the straight morphology associated with their "matrix–twin" nature. A transmission electron microscopic study [23] has shown that straight segments on the long sides of twins in this sample had $\{1\,1\,1\}/\{1\,1\,1\}$ plane indexes, i.e. were coherent twin boundaries. The lengths of twin boundaries separating matrix grains were determined by the size of crystallites within which twinning events occurred.

In strongly textured copper, twin boundaries formed not only between a twin and its matrix (true twin boundaries), but the same twin could form $\Sigma3$ boundaries with neighbours slightly disoriented from the matrix grain (see Fig. 3). Therefore, a wide range of deviations from the exact twin relationship was obtained. The deviations for most "cube neighbour–twin" boundaries were larger than those for true twin boundaries (see Fig. 4). Obviously, many "cube neighbour–twin" boundaries classified as $\Sigma3$ according to Brandon's criterion are unlikely to reveal special properties. Only half of them satisfy a more restrictive $\Delta\theta_c = 15^\circ\ \Sigma^{-5/6}$ criterion [24], where a 6.00° deviation from the ideal twin misorientation is considered as a structural limit for $\Sigma3$ boundaries. Furthermore, such "$\{0\,0\,1\}\langle 1\,0\,0\rangle$ neighbour–twin" boundaries with small deviations from the ideal $\Sigma3$ relationship may not be associated with $\{1\,1\,1\}$ GB planes and therefore, may have a higher GB energy than coherent segments of "matrix–twin" boundaries.

Considering the relative GB lengths of these two groups of boundaries, "matrix–twin" boundaries tend to be longer than $\Sigma3$ boundaries between twins and their non-matrix neighbours. Of course, some twins, e.g. corner twins (see Fig. 3) can form relatively long $\Sigma3$ boundaries with their non-matrix $\{0\,0\,1\}\langle 1\,0\,0\rangle$ neighbours. Nevertheless, more than 60% of the "cube neighbour–twin" $\Sigma3$ boundaries were shorter than 20 μm, while the corresponding fraction of the "matrix–twin" boundaries was only 25%. Apparently during grain growth in the presence of strong texture, the microstructure evolves in such a manner that the low GB energy of straight twin segments permits the persistence of relatively long boundaries. These true twin boundaries are characterized by small deviations from the ideal $\Sigma3$ misorientation. Boundaries between twins and their non-matrix neighbours of a dominant texture component are mostly shorter, can be curved and have larger deviations from the exact $\Sigma3$ misorientation.

5. Conclusions

1. Grain boundary ensembles were investigated in weakly and strongly textured states generated during recrystallization and grain growth in pure copper. It was found that differences in crystallographic texture formed in these conditions markedly influenced the grain boundary distribution.

2. The microstructure with a nearly random distribution of orientations (weak texture) is characterized by a high fraction of $\Sigma3^n (n \geq 1)$ boundaries. Strengthening of the cube $\{0\,0\,1\}\langle 1\,0\,0\rangle$ texture leads to an increase in frequency of low-angle boundaries at the expense of other GBs.

3. The misorientation distribution of nearest neighbours in fcc materials prone to annealing twinning is influenced by the "matrix–twin" orientation correlation. Such a correlation was prominent in weakly textured copper, although all mutual misorientations demonstrated no predominance of $\Sigma3^n$ relationships.

The influence of this orientation correlation may be significantly reduced in the presence of an extremely strong texture. In this case, misorientations between nearest neighbours and all mutual misorientations are determined primarily by the crystallographic texture (dominant cube and its twin component).

4. In strongly textured copper, twins are surrounded by cube-oriented grains. In this state, Σ3 boundaries with different deviations from the ideal Σ3 misorientation are formed around a twin. The morphology of these boundaries appeared to be related to the deviations from the ideal twin relationship. The misorientations across straight "matrix–twin" boundaries were close to the exact twin relationship. Boundaries between twins and their non-matrix neighbours of a dominant texture component are mostly shorter, less linear and generally have larger deviations from the exact Σ3 misorientation.

Acknowledgements

I would like to thank Professor G. Gottstein for provision of laboratory facilities at the Institüte fur Metallkunde und Metallphysik, RWTH Aachen, where the major part of experiments was performed. I am grateful to the Alexander von Humboldt Foundation for supporting my stay in Aachen. A part of this paper was written while I was a visitor at Kanazawa University. Professor K. Kitagawa and the Japan Society for the Promotion of Science are acknowledged for the support of that visit. I would also like to express my gratitude to Dr. V. Y. Gertsman, Dr. D. Juul Jensen and Dr. M. Lyttle for useful discussions.

References

1. A. P. ZHILYAEV, V. Y. GERTSMAN, O. V. MISHIN, A. I. PSHENICHNYUK, I. V. ALEKSANDROV and R. Z. VALIEV, *Acta Metall. Mater.* **41** (1993) 2657.
2. A. MORAVIEC, J. A. SZPUNAR and D. C. HINZ, *ibid.* **41** (1993) 2825.
3. A. GARBACZ and M. W. GRABSKI, *ibid.* **43** (1993) 1541.
4. P. FORTIER, W. A. MILLER and K. T. AUST, *Acta Mater.* **45** (1997) 3459.
5. V. Y. GERTSMAN and K. TANGRI, *Scripta Metall. Mater.* **33** (1995) 1037.
6. V. Y. GERTSMAN, K. TANGRI and R. Z. VALIEV. *Acta Metall. Mater.* **42** (1994) 1785.
7. K. MATSUMOTO, T. SHIBAYANAGI and Y. UMAKOSHI, *Acta Mater.* **45** (1997) 439.
8. L. S. SHVINDLERMAN, V. G. SURSAEVA, V. P. YASHINKOV and R. G. FAULKNER, *Interface Sci.* **2** (1994) 155.
9. Y. PAN and B. L. ADAMS, *Scripta Metall. Mater.* **30** (1994) 1055.
10. T. R. MCNELLEY and M. E. MCMAHON, *Metall. Trans.* **28A** (1997) 1879.
11. O. V. MISHIN, *Scripta Mater.* **38** (1998) 423.
12. D. C. BRANDON, Acta Metall. **14** (1966) 1479.
13. J. K. MACKENZIE, *ibid.* **12** (1964) 223.
14. O. V. MISHIN, *Mater. Sci. Forum* in press.
15. J. K. MACKENZIE, *Biometrika* **45** (1958) 229.
16. D. JUUL JENSEN, *Acta Metall. Mater.* **43** (1995) 4117.
17. O. V. MISHIN and G. GOTTSTEIN, *Mater. Sci. Eng.* **A249** (1998) 71.
18. T. WATANABE, H. FUJII, H. OIKAWA and K. I. ARAI, *Acta Metall.* **37** (1989) 941.
19. T. WATANABE, T. HIRANO, T. OCHIAI and H. OIKAWA, *Mater. Sci. Forum* **157–162** (1994) 1103.
20. V. Y. GERTSMAN, K. TANGRI and O. V. MISHIN, *Interface Sci.* **1** (1993) 157.
21. F. HEIDELBACH, H. R. WENK, S. R. CHEN, J. POSPIECH and S. I. WRIGHT, *Mater. Sci. Eng.* **A215** (1996) 39.
22. V. RANDLE, *Phil. Mag.* **A67** (1993) 1301.
23. O. V. MISHIN and X. HUANG, *Mater. Sci. Forum* in press.
24. G. PALUMBO and K. T. AUST, *Acta Metall. Mater.* **38** (1990) 2343.

Received 30 March
and accepted 30 June 1998